Allosteric Inhibition of PTP1B Activity by Selective Modification of a Non-Active Site Cysteine Residue†

Stig K. Hansen,* Mark T. Cancilla, Timothy P. Shiau, Jenny Kung, Teresa Chen, and Daniel A. Erlanson*

Sunesis Pharmaceuticals, Inc., 341 Oyster Point Boulevard, South San Francisco, California 94080

Received December 8, 2004; Revised Manuscript Received March 17, 2005

ABSTRACT: The fluorogenic reagent 4-(aminosulfonyl)-7-fluoro-2,1,3-benzoxadiazole (ABDF) attenuates the functional activity of the protein tyrosine phosphatase PTP1B by reacting selectively with a single cysteine residue, leaving other cysteines in the protein unmodified. This modification reduces V_{max} without substantially affecting substrate binding (K_m), indicative of an allosteric mode of inhibition. Consistent with this, the cysteine residue modified by ABDF, Cys 121, lies outside the catalytic site but makes interactions with residues that contact His 214, which has been shown to be important for catalysis. Cys 121 is highly conserved among phosphatases, and ABDF also inhibits TC-PTP and LAR. These findings illustrate that targeting cysteine residues outside catalytic sites may be exploited in allosterically regulating enzymes. Moreover, these results suggest a new strategy for inhibiting a promising diabetes target.

The protein tyrosine phosphatase PTP1B[1] is an exciting target for the treatment of type II diabetes and obesity (*1*). The enzyme is a negative regulator of the insulin signaling pathway, acting presumably by dephosphorylating phosphotyrosine residues in the insulin receptor and/or insulin receptor substrate. The catalytic mechanism involves direct attack of the active site cysteine in PTP1B on the phosphate group of phosphotyrosine, followed by hydrolysis of the intermediate phosphocysteine (*2*, *3*).

Inhibitors of PTP1B generally fall into two categories: phosphotyrosine mimetics and covalent inactivators (*4*). The first category has received the most attention; numerous phosphotyrosine mimetics have been reported, and many have been elaborated to obtain specific, high-affinity inhibitors against PTP1B (*5*, *6*).

The second category of inhibitors consists largely of reactive molecules which modify the active site cysteine. Chief among these are Michael acceptors, including naphthoquinones such as vitamin K3 (menadione) (*7*, *8*). A related analogue is reported to selectively inactivate PTP1B with a k_{inact} constant of 1.3 min^{-1} (*9*). Halomethyl ketones also alkylate PTP1B with k_{inact} constants in the range of 0.6 min^{-1} (*10*). Widlanski has reported a mechanism-based phosphatase inhibitor that is converted to a highly reactive quinone methide capable of labeling the enzyme (*11*), and generic electrophiles such as epoxides have also been reported to inhibit phosphatases (*12*).

Surprisingly, combining these two categories of inhibitors has been challenging: many phosphotyrosine mimetics designed to be irreversible modifiers, such as tyrosine epoxides and chloromethylphosphonates, have not shown activity against thiol phosphatases (*13*). However, halobenzylphosphonates are a notable exception (*14*). In fact, these electrophiles seem to be highly selective for cysteine protein tyrosine phosphatases while being completely inert to common nucleophiles such as azide and cysteine, demonstrating the reactivity of the active site cysteine (*15*). Small molecules such as quinones and pyridazines have been reported to oxidize the active site cysteine (*16*−*18*), and the active site cysteine can be oxidized under very mild conditions to form a sulfenamide (*19*, *20*), a finding which may reflect a regulatory mechanism in vivo (*21*).

As part of our Tethering (*22*, *23*) with Extenders technology platform (*24*, *25*), we sought small molecule probes that react specifically and irreversibly with the active site cysteine of PTP1B. We use electrospray mass spectrometry to screen potential compounds; covalent modifiers will alter the mass of the protein to reveal both the extent and stoichiometry of labeling. The native PTP1B enzyme contains five free cysteine residues in addition to the active site, and at least two of these are surface-exposed and thus potentially reactive to small molecules. Indeed, previous work had shown that treatment of PTP1B with oxidized glutathione resulted in disulfide formation with two or three cysteines per molecule of PTP1B (*26*). In our hands as well, screening a wide variety of potential electrophiles revealed that most of these alkylate the protein at multiple sites. However, we discovered that 4-(aminosulfonyl)-7-fluoro-2,1,3-benzoxadiazole [ABDF (*27*), Figure 1] reacts rapidly and selectively with a single cysteine residue on the enzyme.

ABDF is a thiol-selective fluorogenic modifier that is only weakly fluorescent until it reacts with thiols. It has been used for identifying and quantifying low-molecular weight thiols

† Supported in part by Small Business Innovative Research Grant R43-DK063764.

* To whom correspondence should be addressed. Phone: (650) 266-3668 (S.K.H.) or (650) 266-3607 (D.A.E.). Fax: (650) 266-3501. E-mail: hansen@sunesis.com or erlanson@sunesis.com.

[1] Abbreviations: ABDF, 4-(aminosulfonyl)-7-fluoro-2,1,3-benzoxadiazole; ESI-MS, electrospray ionization mass spectrometry; pNPP, *p*-nitrophenyl phosphate; PTP, protein tyrosine phosphatase; PTP1B, protein tyrosine phosphatase 1B; TCPTP, T-cell protein tyrosine phosphatase.

10.1021/bi047417s CCC: $30.25
Published on Web 05/07/2005

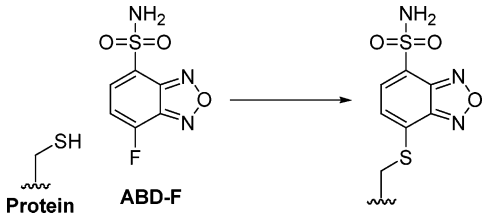

FIGURE 1: Mechanism of cysteine reaction with ABDF.

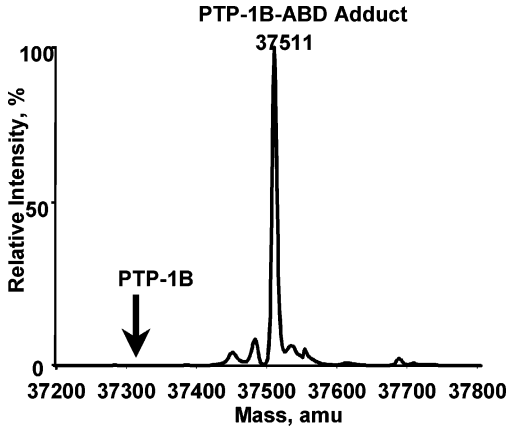

FIGURE 2: Deconvoluted, neutral-scale ESI mass spectrum of ABD-modified PTP1B. The protein is completely modified by one ABD moiety. The arrow indicates the mass at which unlabeled PTP1B would be present.

as well as for quantifying and mapping the positions of free cysteine residues and disulfide bonds in peptides and proteins (*27*−*31*). Compared with other thiol-reactive probes, ABDF shows attenuated reactivity, and some cysteine residues are modified preferentially over other cysteines in a given protein (*32*, *33*). This selectivity has facilitated its use as an environmentally sensitive fluorescent probe in mobile regions of proteins (*34*−*38*). The benzoxadiazole fluorophore has also been used in fluorescence resonance energy transfer (FRET) studies to study membrane proteins (*39*). Given the reactivity of the active site cysteine in PTP1B, we initially believed that ABDF selectively modifies the catalytic cysteine. As we show below, ABDF actually modifies a cysteine residue some distance from the active site and allosterically inhibits PTP1B.

MATERIALS AND METHODS

Biochemical Assays. Cloning and protein expression were performed as previously described (*40*). Two constructs of PTP1B were used, a 298-amino acid version and a 321-amino acid version, differing only in their C-terminal residues. These have comparable activities, and the added 23 amino acids of the longer version do not include cysteine residues. For most experiments, the longer construct was used; however, for the data in Figure 3A, the shorter version was used. Activity assays with substrate *p*-nitrophenyl phosphate (pNPP) were conducted using 100 or 200 nM PTP1B essentially as described previously (*40*). In general, 5 mM pNPP was used as the substrate, except where noted in the figure legend. For kinetic assays, the $A_{405} - A_{655}$ difference was determined every 11 s and rates were calculated over 60 s intervals. All reactions were carried out at ambient temperature. For reversibility experiments, PTP1B was labeled as described below and excess ABDF was removed

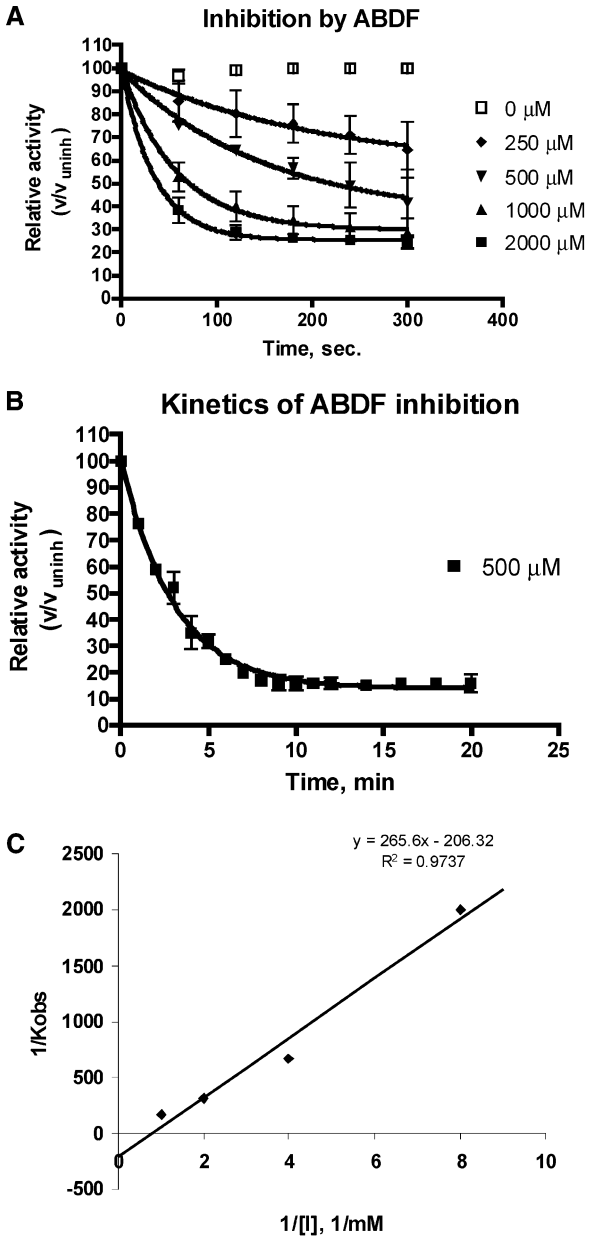

FIGURE 3: (A) ABDF shows time- and concentration-dependent inhibition of PTP1B. Every minute, rates were calculated as the average rate during the preceding 60 s and normalized relative to an uninhibited control. Curve fitting was according to a one-phase exponential decay (GraphPad Prism). $R^2 = 0.979$ (250 μM), 0.992 (500 μM), 0.997 (1000 μM), and 0.999 (2000 μM). The concentration of PTP1B was 200 nM. (B) ABDF inhibition of PTP1B plateaus at ~14% residual activity. Rates were calculated every minute as in panel A and normalized relative to an uninhibited control. The concentration of PTP1B was 100 nM. Protein was more than 99% labeled after incubation for 10 min. Data were fitted to a one-phase exponential decay with a half-life of 2.1 min. $R^2 = 0.993$. (C) Kitz−Wilson plot of initial rates vs ABDF concentration. Rates (k_{obs}) were determined during the initial 200 s of the inactivation reaction and as the slope of log(% activity) vs time (semilog plot of data in panel A). The *y*-intercept is $1/k_{inact}$, and the *x*-intercept is $1/K_i$. The value of k_{inact} is 4.9×10^{-3} s^{-1}, and the value of K_i is 1.3 mM. The concentrations of ABDF were 125, 250, 500, and 1000 μM.

on a NAP-5 desalting column (Amersham Pharmacia Biotech). PTP1B (5 μM) was incubated in the presence of 100 mM DTT for 0, 1, 2, 3, 4, or 5 h. Following the incubation, samples were removed for functional assays (final PTP1B

concentration of 250 nM) and mass spectrometry. For kinetic studies, 200 nM PTP1B (labeled and unlabeled) was incubated with varying concentrations of pNPP substrate (see figure legends for details). Data were fitted by nonlinear regression analysis according to a Michaelis−Menten kinetic model (GraphPad Prism version 4.01).

TCPTP was cloned, expressed, and purified as previously described (*40*). CD45 and LAR were purchased from Calbiochem and exchanged into 100 mM Tris (pH 7.0) using a Nap-5 column. TCPTP (final concentration of 150 nM), CD45 (final concentration of 130 nM), and LAR (final concentration of 110 nM) were treated with ABDF (final concentration of 1 mM) and pNPP (final concentration of 5 mM). A_{410} was determined every 10 s, and rates were calculated over 60 s intervals (for TCPTP) or over 300 s intervals (for CD45 and LAR). The data were not corrected for a minor contribution of the ABD−cysteine adduct to the absorbance at 410 nm ($\epsilon_{410} \sim 5000\ cm^{-1}\ M^{-1}$).

Fluorescence Polarization Assay. Fluorescein-labeled peptide, FAM-DADEY(PO_3)L-NH_2, was dissolved at 200 μM in DMSO and diluted to 1 nM in assay buffer [50 mM Hepes (pH 7.0), 100 mM NaCl, 1 mM EDTA, 0.1 mg/mL Bovine IgG, and 0.005% Triton X-100]. A PTP1B dilution series (from 100 to 0.4 nM) was made in the same buffer. Diluted peptide (50 μL) and 50 μL of PTP1B were mixed in black, flat-bottom microtiter plates. The mixture was incubated at ambient temperature for 10 min with gentle shaking before readings were taken in an Analyst LJL instrument. Data were fitted according to a one-site binding model (GraphPad Prism version 4.01).

Cell-Based Assays. CHO-hIR cells were plated at 60% confluency in six-well plates approximately 16 h prior to compound treatment. Cells were grown in DMEM with 10% FBS supplemented with antibiotic/antimycotic (1:100 dilution) and G418 (1:100 dilution). ABDF was diluted in media and incubated with cells for 30 min at 37 °C. Pervanadate was complexed to phenanthroline [bpV(phen), Calbiochem catalog no. 206395]. Five minutes prior to lysis, 5 nM insulin was added where specified. Cell lysates were prepared as described previously (*40*). Phosphopeptide specific antibodies were purchased from Biosource. The protein concentration was determined by the BCA protein assay (Pierce), and 10 μg of protein was loaded per lane and analyzed by Western blot analysis.

Modification of PTP1B with ABDF. PTP1B was exchanged into 100 mM Tris (pH 7.0) using a Nap-5 column and reacted with excess ABDF (dissolved in DMSO); typical concentrations were 26 μM PTP1B and 500 μM ABDF. The reaction was generally complete within 1 h as judged by mass spectrometry (see below). Excess ABDF was removed using a Nap-5 column. The protein concentration was quantified using the reported extinction coefficient for the ABD−cysteine adduct ($\epsilon_{385} = 7800\ cm^{-1}\ M^{-1}$) (*41*) as well as that calculated for PTP1B ($\epsilon_{280} = 1.33\ cm^{-1}\ M^{-1}$); the two methods produced identical values to within 5%.

Digestion and Characterization of Modified PTP1B. Intact mass determination of PTP1B modified with ABDF was carried out using a QSTAR Pulsar i quadrupole time-of-flight mass spectrometer (Applied Biosystems/MDS Sciex, Foster City, CA) equipped with a LEAP HTS autosampler (LEAP Technologies, Carrboro, NC) and an HP1100 gradient pump (Agilent Technologies, Palo Alto, CA). On-line protein desalting was performed with a protein μ-trap (Michrom BioResources, Auburn, CA) with a gradient of 5% B for 30 s, ramped to 95% B by 0.7 s, and held at 95% B until 1.5 min before returning to the initial conditions by 1.7 min (mobile phase A being 0.1% formic acid and mobile phase B being 0.1% formic acid in acetonitrile) running at 600 μL/min split down to 35 μL/min before the introduction into the electrospray ionization (ESI) source. The mass spectrometer was operated with an ESI voltage of 5000 V, a declustering potential of 60 V, a focusing potential of 260 V, and a scan accumulation time of 1.0 s. Intact protein mass spectra were deconvoluted using Bayesian protein reconstruct within BioAnalyst software to obtain a neutral scale (zero-charge) mass spectrum.

For tryptic digestion of the PTP1B−ABD adduct, it was denatured with an equal volume of a 0.2% solution of the acid-labile anionic surfactant, RapiGest SF (Waters, Milford, MA), to yield a 30 μM PTP1B−ABD solution that was 0.1% RapiGest SF. Proteomics grade trypsin (Promega, Madison, WI) was added to give a desired trypsin:protein ratio of 1:50 (w/w) and digested for 60 min at 37 °C. The RapiGest SF was removed by adding HCl to a final concentration of 50 mM (pH ∼2). The acidified peptide solution was centrifuged at 13 000 rpm for 10 min, and the bottom aqueous layer was loaded off-line onto a μ-peptide trap (Michrom BioResources) and washed with 1 mL of 0.1% FA. Peptides were eluted from the trap with 1 mL of 90% acetonitrile and 0.1% formic acid and vacuum centrifuged to remove the organic solvent followed by lyophilization. The peptides were redissolved in 50 μL of 20% acetonitrile and 0.1% formic acid, and 10 μL was loaded into 0.94 mm inside diameter GlassTip emitter (New Objective, Woburn, MA) for nanoelectrospray (nanoES) analysis. The mass spectrometer was operated with a capillary voltage of 1250 V, a declustering potential of 40 V, a focusing potential of 350 V, and a scan accumulation time of 2.0 s. Collision-induced dissociation of peptides was performed at a collision energy of 35 V using nitrogen as the collision gas. All nanoES mass spectra were accumulated for 5 min.

RESULTS

We reacted PTP1B with ABDF and discovered (by using ESI mass spectrometry) that ABDF rapidly and quantitatively modified the enzyme at a single site (theoretical mass of 37 510 amu, observed mass of 37 511 amu), even in the presence of a large excess of ABDF (Figure 2). As noted above, PTP1B contains five cysteine residues in addition to the active site cysteine. Because of the reactivity of the active site Cys 215, we initially assumed that this was the modified residue.

To determine the effects of this modification on catalysis, we ran enzymatic assays in the presence of ABDF. As shown in Figure 3A, ABDF inhibited PTP1B in a concentration- and time-dependent manner. To determine the kinetics of the reaction, enzyme activity in the presence of 500 μM ABDF was monitored continuously over a period of 20 min (Figure 3B). The data can be fitted to one-phase exponential decay ($R^2 = 0.993$) with a half-life of 126 s or a rate constant of $5.5 \times 10^{-3}\ s^{-1}$. Kinetic data were also examined using a Kitz−Wilson reciprocal plot of the rate constants that can be derived from a semilog version of the data in Figure 3A

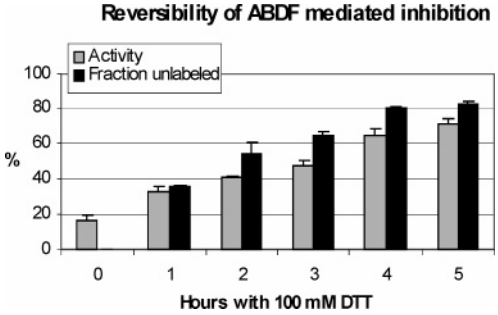

FIGURE 4: Reversibility of ABDF inhibition. PTP1B, which was quantitatively labeled with ABDF, was incubated with DTT for the indicated period of time. At the end of each incubation, PTP1B activity was determined in a functional assay and the ratio of unlabeled to labeled protein was determined by mass spectrometry. The data points are the average of three determinations.

(Figure 3C). The values for K_i and the inactivation rate constant k_{inact} are 1.3 mM and 4.9×10^{-3} s^{-1} (0.29 min^{-1}), respectively. Surprisingly, the inhibition curve in Figure 3B plateaus at 14% residual activity, even though the protein was quantitatively labeled within 10 min, suggesting that conjugation with ABDF leads to only partial (approximately 86%) inactivation. This was confirmed by monitoring residual activity for up to 2.5 h, showing no additional reduction in activity (data not shown). These observations suggest that ABDF reacts with a residue other than the catalytic cysteine (see below), since quantitative labeling of the catalytic cysteine would result in complete inactivation. Thus, ABDF is not a classical mechanism-based inhibitor.

The thioether that forms when ABDF reacts with cysteine has been reported to be reversible (*41*, *42*), and we found that incubation with DTT led to recovery of enzymatic activity. Reversibility was monitored for 5 h by both enzyme assay and mass spectrometry (Figure 4), revealing that enzymatic activity was recovered as the ABD moiety was removed. The reversal was slow, showing a restoration of 50% of full activity after ~3 h. Complete removal of the ABD moiety required a 20 h incubation and resulted in an ~90% recovery of enzymatic activity (data not shown). Interestingly, although the ABD adduct has been shown to be only partly reversible in the case of serum albumin (*41*), here we see almost complete regeneration of the native enzyme activity.

To determine the mechanism of inhibition, we conducted a substrate titration experiment using both unlabeled and fully labeled PTP1B. This analysis revealed that conjugation with ABDF resulted in a 7.4-fold decrease in V_{max} with an only modest effect on K_m, demonstrating that binding of ABDF interferes with catalytic activity rather than substrate binding (Figure 5A). To confirm this observation, we conducted a binding study using PTP1B and a fluorescently labeled peptide, DADEY(PO_3)L, corresponding to residues 988−993 of the human EGF receptor (*43*). This analysis revealed that peptide binding was not substantially affected by labeling with ABDF [K_d = 8.4 nM with ABDF, and K_d = 5.6 nM without ABDF (Figure 5B)]. In addition, we found that ABDF modification was not affected by the presence of the active site binder Na_3VO_4 (data not shown), suggesting that ABDF binding occurs outside the active site. Taken together, these data suggest that ABDF reacts with a residue other than the catalytic C215 and inhibits the enzyme by interfering

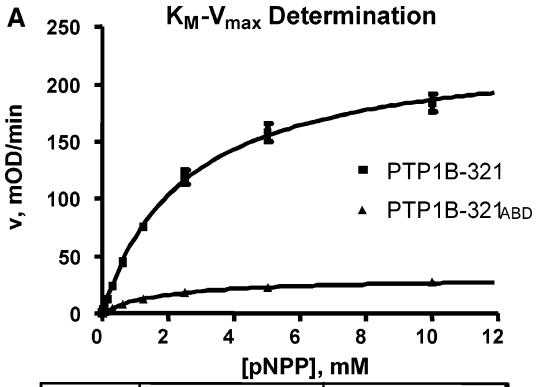

	PTP1B-321	PTP1B-321ABD
V_{max}	234	31.5
K_M	2.5	1.8

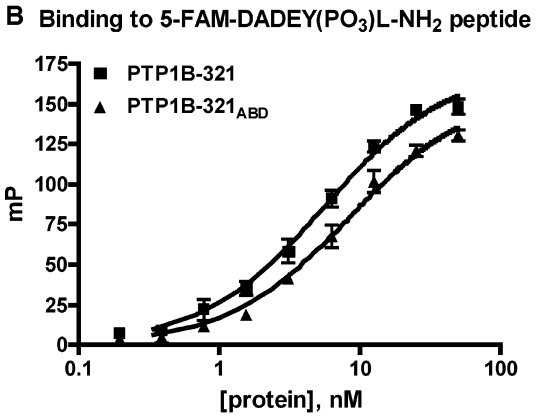

	PTP1B-321	PTP1B-321ABD
B_{max}	172	158
K_d	5.6	8.4

FIGURE 5: (A) Noncompetitivity of ABDF inhibition. Determination of K_m and V_{max} for ABD-labeled and unlabeled PTP1B. Substrate pNPP was titrated from 0.08 to 10 mM. Averages of three determinations were fitted by nonlinear regression analysis (R^2 = 0.996 for PTP1B and 0.999 for PTP1B−ABD). (B) ADB-labeled PTP1B binds the substrate peptide. Determination of binding affinity of ABDF-labeled PTP1B for a phosphopeptide derived from the EGF receptor. Binding affinity was determined by fluorescence polarization using a D181A mutant form of PTP1B. Protein labeling (>99%) was confirmed by mass spectrometry. Data show the average of three determinations and were fitted according to a one-site binding mechanism (R^2 = 0.997 for PTP1B-D181A and 0.995 for ADB-labeled PTP1B-D181A).

with catalytic function, probably through an allosteric mechanism.

The results described above suggest that ABDF targets not the active site cysteine but one of the five other cysteine residues in our PTP1B construct. Moreover, recent data suggest that ABDF can label residues besides cysteine (*44*). To find the reactive residue, we performed peptide mapping experiments on the modified protein. As seen above, ABDF modification of cysteine residues is reversible under reducing conditions (*41*), so to prevent possible scrambling of the

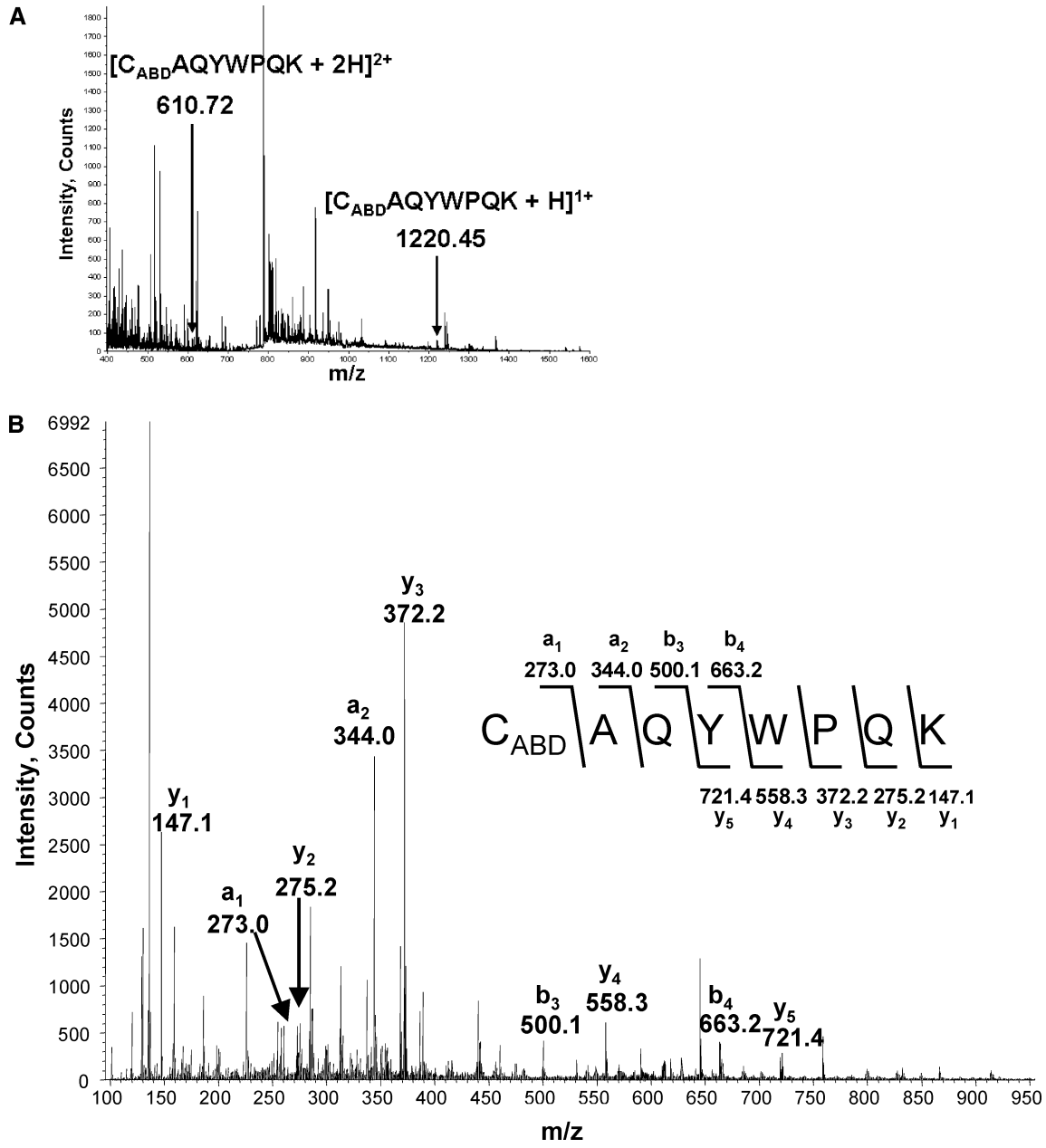

FIGURE 6: (A) Nano-ESI mass spectrum of the total PTP1B−ABD tryptic peptide mixture. Both the $[M + H]^+$ and $[M + 2H]^{2+}$ ions of ABD-modified tryptic peptide 121−128 are clearly visible. (B) Collision-induced dissociation mass spectrum of the $[M + 2H]^{2+}$ ion at *m*/*z* 610.72. The a-, b-, and y-type fragment ions that were generated confirm the sequence of the peptide and the location of the ABD moiety on Cys 121. Only sequence specific ions are labeled for clarity.

label, we reacted the ABDF-modified protein with iodoacetamide to alkylate all other cysteine residues followed by tryptic digestion.

Figure 6A shows the nano-electrospray mass spectrum of the total peptide mixture produced from the digested protein. Despite the large number of ions corresponding to numerous peptides, the singly and doubly charged ions corresponding to an ABD-modified peptide comprising residues 121−128 are clearly visible at *m*/*z* 1220.45 and 610.72, respectively. The observed mass of this peptide agrees with the theoretical mass to within 8 ppm (Table 1) with external calibration. We also looked for ABD modification on the other cysteine-containing peptides resulting from the digest; we found that all of the other cysteine residues were modified by iodoacetamide (forming the carboxyamidomethyl moiety, CAM) and could be accounted for (Table 1). We also did not observe peptide 121−128 with the CAM modification (data not shown). To further confirm the location of the ABD modification, collision-induced dissociation was performed on the $[M + 2H]^{2+}$ ion at *m*/*z* 610.72 as shown in Figure 6B. The a-, b-, and y-type fragment ions that were generated verify the sequence of the tryptic peptide and show clearly

Table 1: Sequences and Observed and Calculated Masses of Peptides Derived from ABD-Modified, Tryptic-Digested PTP1B[a]

Cys Containing Tryptic Peptide	Sequence	Observed Mass	Theoretical Mass
25 - 33	HEASDFPC$_{Cam}$R	1117.45	1117.46
80 - 103	SYILTQGPLPNTC$_{Cam}$GHFWEMVWEQK	2920.35	2920.37
121 – 128	C$_{ABD}$AQYWPQK	1219.44	1219.45
200 - 221	ESGSLSPEHGPVVVHC$_{Cam}$SAGIGR	2231.1	2231.07
222 – 237	SGTFC$_{Cam}$LADTC$_{Cam}$LLLMDK	1843.87	1843.85

[a] Cam is carboxyamidomethyl.

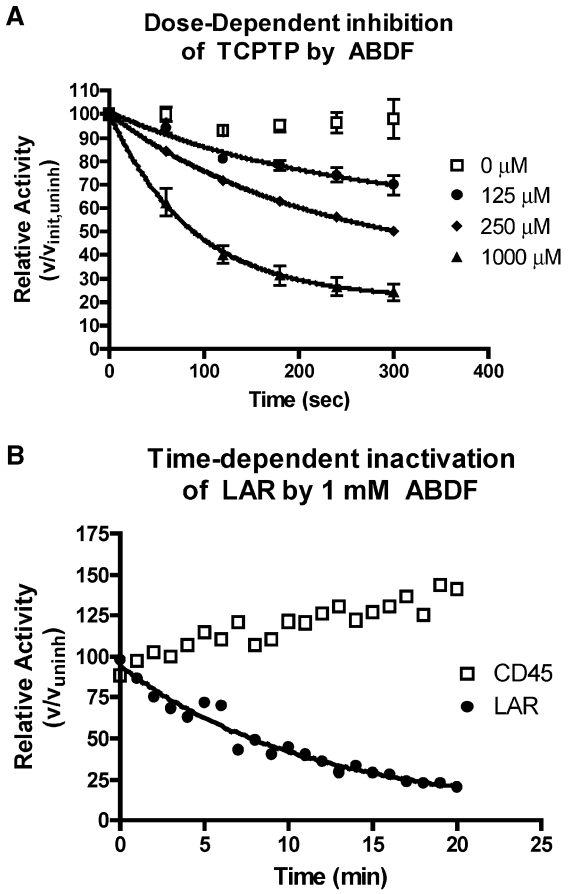

FIGURE 7: (A) ABDF shows time- and concentration-dependent inhibition of TCPTP (150 nM). Rates were calculated and fitted as in Figure 3A, and normalized relative to the initial velocity of the uninhibited control. $R^2 = 0.9595$ (1000 μM), 0.9850 (250 μM), and 0.8813 (125 μM). Mass spectral analysis of the reaction of TCPTP with 1 mM ABDF and 5 mM pNPP at 5 min showed greater than 90% single modification (data not shown). (B) LAR (110 nM) shows time-dependent inactivation by ABDF, while CD-45 is not inhibited. Rates were calculated every minute as in panel A and normalized relative to an uninhibited control. The curve for LAR was fit to a one-phase exponential decay (GraphPad Prism). $R^2 = 0.9683$.

that ABDF has modified Cys 121. In summary, the peptide digestion experiments reveal that ABDF modifies PTP1B not at the highly reactive active site cysteine (Cys 215) but at a cysteine residue nearly 10 Å away not previously seen to be reactive.

We also investigated whether ABDF was specific to PTP1B, or whether ABDF also inhibits other protein tyrosine phosphatases. Given the electrophilic mechanism of action and the near-universal conservation of Cys 121 and residues in the vicinity (Tyr 124 and Lys 120), ABDF would be expected to react with other phosphatases. Indeed, ABDF inhibits the closely related TCPTP in a time- and concentration-dependent manner (Figure 7A). LAR is also inhibited by ABDF, but interestingly, CD45 is not inhibited, indicating that there is some degree of sequence specificity toward inhibition by ABDF (Figure 7B).

Since PTP1B, TCPTP, and LAR have been implicated as potential negative regulators of insulin signaling, we were interested in determining whether ABDF could stimulate insulin receptor phosphorylation in cells. Addition of ABDF to CHO-hIR cells caused a dose-dependent increase in the

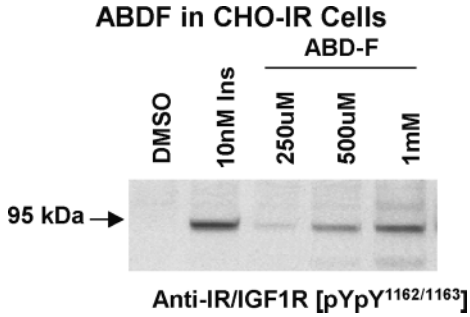

FIGURE 8: Whole cell lysates were examined by Western blot analysis using an anti-hIR/IGF1R-[pYpY1162/1162] antibody. Cells were treated with insulin for 5 min and with ABDF for 30 min in the presence of 10% serum. The migration of the IR β-subunit is denoted with an arrow.

level of insulin receptor phosphorylation (Figure 8). The specific phosphorylation of the insulin receptor was confirmed by Western blot analysis, showing that ABDF treatment stimulates phosphorylation of tyrosines 1162 and 1163 of the activation loop of the insulin receptor. The level of receptor phosphorylation with the highest ABDF concentration was comparable to that seen with insulin alone. These data are consistent with inhibition of PTP1B, TC-PTP, and LAR, although the precise role of each of these phosphatases cannot be determined from these experiments. Taken together, our data show that targeting Cys 121 in PTP1B could be a valuable mechanism for inhibiting PTP1B with potential utility in stimulating insulin receptor signaling.

DISCUSSION

We have demonstrated that ABDF reacts selectively with a single cysteine residue, Cys 121, on PTP1B. This modification decreases the enzymatic activity of PTP1B in vitro, and ABDF activates the insulin signaling pathway in cells, although the precise mechanism of this activation may not be due solely to PTP1B inhibition. The specificity of ABDF for Cys 121 is surprising for several reasons. First, as discussed above, the active site cysteine of any PTP is highly reactive, with a pK_a of ~5 (*45*). Moreover, PTP1B has two surface cysteine residues, Cys 32 and Cys 92, which are highly exposed to solvent and would be expected to be reactive (Figure 9A). Indeed, most electrophiles that we have reacted with PTP1B produce multiple labelings, likely due to modification of these cysteine residues. In contrast, the side chain of Cys 121 points toward the interior of the protein, suggesting that some sort of rearrangement is necessary to accommodate the binding of ABDF. Our kinetic studies show that this rearrangement results in decreased catalytic activity while substrate binding is largely unaffected. Together, these observations suggest that ABDF inhibits catalytic activity through an allosteric mechanism, probably by inducing a low-activity conformation of PTP1B. Unfortunately, we have been unable to crystallize ABD-modified PTP1B to determine the precise binding mode, despite the fact that unmodified PTP1B crystallizes readily.

How does the modification of Cys 121 reduce the activity of PTP1B? Recently, we have reported small molecule compounds that can allosterically inhibit PTP1B by binding to a site some 20 Å from the active site [and more than 25 Å from Cys 121 (Figure 9B)]. These allosteric inhibitors block the mobility of the catalytic "WPD" loop, thereby

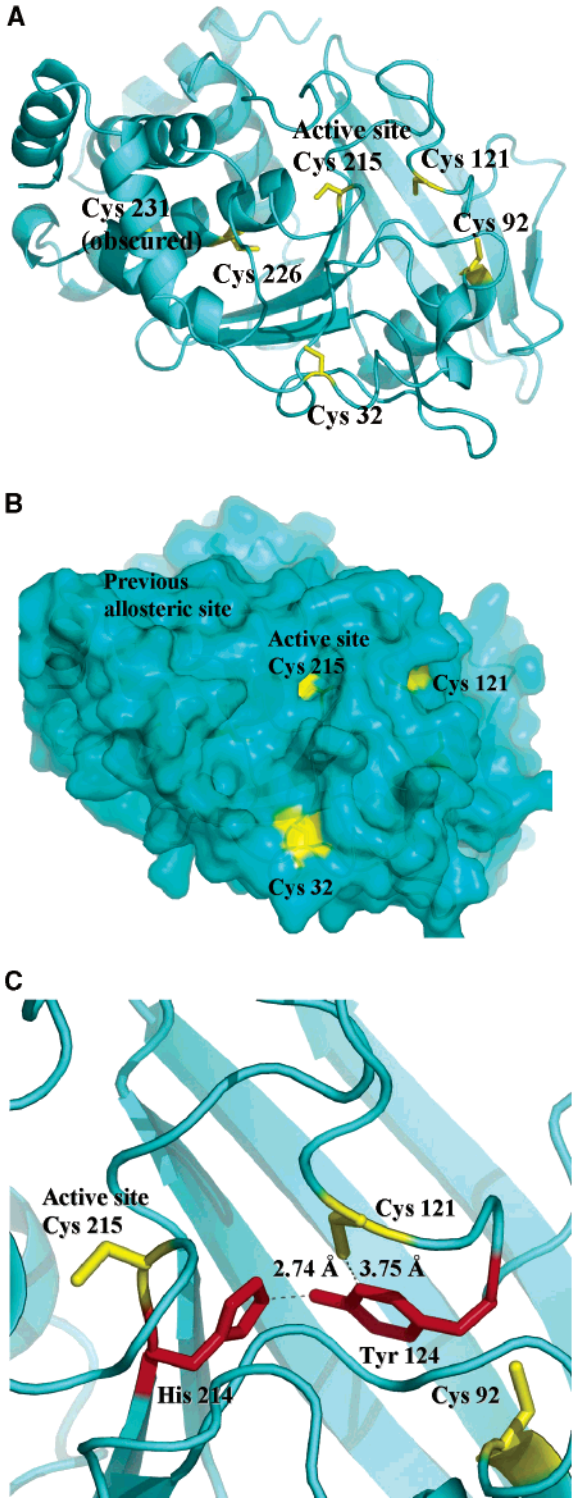

FIGURE 9: (A) Cartoon structure of PTP1B showing the cysteine residues, including the active site cysteine Cys 215 and the ABD-modified cysteine Cys 121. The structure was taken from PDB entry 2HNP (*54*). (B) Same view as in panel A, except with the surface visible. Cys 121 is clearly pointed toward the interior of the protein. The allosteric site previously reported (*40*) is also labeled. (C) Close-up view of the region around Cys 121 showing the proximity of the Tyr 124−His 214 salt bridge. All panels were made using PyMol (*55*).

preventing formation of the active form of the enzyme (*40*). However, comparing a number of structures of PTP1B reveals that Cys 121 is not implicated in this allosteric change, indicating that the mechanism of ABDF inhibition is likely different. Interestingly, Cys 121 is conserved in most PTPs and is part of the conserved motif 7 that is adjacent to the catalytic site (*46*). Cys 121 is only 8.1 Å from the catalytic Cys 215 (distance between Cα atoms), and the sulfur atom packs against the side chain of Tyr 124, which in turn forms a hydrogen bond with His 214, the residue preceding the active site Cys 215 (Figure 9C). Introducing the ABD functionality onto the cysteine would disrupt this delicate packing arrangement, thereby perturbing the active site. In support of this model, it has been shown that mutation of His 214 severely impairs catalytic activity (80−90-fold drop in V_{max}) but somewhat improves substrate binding (5-fold drop in K_m) (*47*). This supports our observation that ABDF inhibits PTP1B by lowering catalytic activity (V_{max}) rather than affecting substrate binding. Of course, in the absence of a crystal structure, it is difficult to determine the precise mode of action; it is still possible that the ABD modification causes a reduced mobility of the WPD loop, in analogy to the previously discovered class of inhibitors. If so, this would be all the more interesting given the large distance between Cys 121 and the previously identified allosteric site.

The specificity of ABDF toward PTP1B is only partial, but it is intriguing, particularly given the fact that Cys 121 is conserved in most PTPs. While phosphatases TCPTP and LAR are inhibited by ABDF, CD45 shows no inhibition. Clearly, even partial inhibition of other PTPs complicates interpretation of cell data, but these differences do raise the hope that more specific compounds would be achievable through medicinal chemistry.

The results presented here raise the interesting possibility that targeting a natural cysteine in PTP1B could be exploited to control enzyme activity. Regulation of protein activity by cysteine modification or disulfide bond formation has been demonstrated in several cases and is believed to mediate cellular responses to oxidative stress (*48*−*52*). Recently, Hardy et al. have reported that a conserved cysteine residue in a deep cavity of caspases can react with a disulfide-containing small molecule to allosterically inhibit enzymatic activity (*53*). Crystallographic characterization of this modification revealed that the bound compound induces a conformational change that precludes substrate binding; indeed, the cysteine-conjugated protein is more similar to the zymogen form of the enzyme. In the case of the caspases, the modified cysteine residue sits at the bottom of a large concave pocket, while in the case of PTP1B, Cys 121 is buried beneath the surface of the protein. Moreover, disulfide modification of the allosteric cysteine residue in caspases changes the conformation sufficiently that substrate can no longer bind, while ABD modification of Cys 121 in PTP1B still allows substrate binding. Nevertheless, these two systems illustrate that targeting natural cysteines can inhibit enzyme activity through different allosteric mechanisms. While the cysteines in PTP1B and caspases may merely represent cryptic allosteric sites, it seems plausible that proteins could have evolved ancillary cysteine residues that regulate protein activity. In either case, targeting natural cysteines could become a valuable method for uncovering new approaches for inhibiting enzyme activity.

In summary, we have found that the small molecule ABDF specifically alkylates a non-active site cysteine of PTP1B and attenuates activity both in vitro and in cells. This

discovery reveals a new mode of inhibiting this important therapeutic target. Although covalent inhibitors are generally viewed disapprovingly as drug candidates, the remarkable specificity of ABDF for Cys 121 as well as its reversibility suggests an alternative drug discovery approach.

ACKNOWLEDGMENT

We thank Jeanne A. Hardy and James A. Wells for helpful comments on the manuscript and Monya L. Baker for editorial assistance.

REFERENCES

1. Andersen, J. N., and Tonks, N. K. (2004) in *Topics in Current Genetics* (Arino, D. R. A., Ed.) pp 201−230, Springer-Verlag, Berlin.
2. Zhang, Z. Y. (2002) Protein tyrosine phosphatases: Structure and function, substrate specificity, and inhibitor development, *Annu. Rev. Pharmacol. Toxicol. 42*, 209−234.
3. Tonks, N. K., and Neel, B. G. (2001) Combinatorial control of the specificity of protein tyrosine phosphatases, *Curr. Opin. Cell Biol. 13*, 182−195.
4. Moller, N. P. H., Iversen, L. F., Andersen, H. S., and McCormack, J. G. (2000) Protein tyrosine phosphatases (PTPs) as drug targets: Inhibitors of PTP-1B for the treatement of diabetes, *Curr. Opin. Drug Discovery Dev. 3*, 527−540.
5. Burke, T. R., Jr., Yao, Z. J., Liu, D. G., Voigt, J., and Gao, Y. (2001) Phosphoryltyrosyl mimetics in the design of peptide-based signal transduction inhibitors, *Biopolymers 60*, 32−44.
6. Johnson, T. O., Ermolieff, J., and Jirousek, M. R. (2002) Protein tyrosine phosphatase 1B inhibitors for diabetes, *Nat. Rev. Drug Discovery 1*, 696−709.
7. Ham, S. W., Park, J., Lee, S.-J., Kim, W., Kang, K., and Choi, K. H. (1998) Naphthoquinone analogs as inactivators of cdc25 phosphatase, *Bioorg. Med. Chem. Lett. 8*, 2507−2510.
8. Ni, R., Nishikawa, Y., and Carr, B. I. (1998) Cell growth inhibition by a novel vitamin K is associated with induction of protein tyrosine phosphorylation, *J. Biol. Chem. 273*, 9906−9911.
9. Ham, S. W., Park, J., Lee, S. J., and Yoo, J. S. (1999) Selective inactivation of protein tyrosine phosphatase PTP1B by sulfone analogue of naphthoquinone, *Bioorg. Med. Chem. Lett. 9*, 185−186.
10. Arabaci, G., Xiao-Chuan, G., Beebe, K. D., Coggeshall, K. M., and Pei, D. (1999) α-Haloacetophenone derivatives as photoreversible covalent inhibitors of protein tyrosine phosphatases, *J. Am. Chem. Soc. 121*, 5085−5086.
11. Myers, J. K., and Widlanski, T. S. (1993) Mechanism-based inactivation of prostatic acid phosphatase, *Science 262*, 1451−1453.
12. Zhang, Z.-Y., Davis, J. P., and Van Etten, R. L. (1992) Covalent modification and active site-directed inactivation of a low molecular weight phosphotyrosyl protein phosphatase, *Biochemistry 31*, 1701−1711.
13. Bobko, M., Wolfe, H. R., Saha, A., Dolle, R. E., Fisher, D. K., and Higgins, T. J. (1995) CD45 protein tyrosine phosphatase: Determination of minimal peptide length for substrate recognition and synthesis of some tyrosine-based electrophiles as potential active-site directed irreversible inhibitors, *Bioorg. Med. Chem. Lett. 5*, 353−356.
14. Taylor, W. P., Zhang, Z.-Y., and Widlanski, T. S. (1996) Quiescent affinity inactivators of protein tyrosine phosphatases, *Bioorg. Med. Chem. 4*, 1515−1520.
15. Kumar, S., Zhou, B., Liang, F., Wang, W. Q., Huang, Z., and Zhang, Z. Y. (2004) Activity-based probes for protein tyrosine phosphatases, *Proc. Natl. Acad. Sci. U.S.A. 101*, 7943−7948.
16. Guertin, K. R., Setti, L., Qi, L., Dunsdon, R. M., Dymock, B. W., Jones, P. S., Overton, H., Taylor, M., Williams, G., Sergi, J. A., Wang, K., Peng, Y., Renzetti, M., Boyce, R., Falcioni, F., Garippa, R., and Olivier, A. R. (2003) Identification of a novel class of orally active pyrimido[5,4-3][1,2,4]triazine-5,7-diamine-based hypoglycemic agents with protein tyrosine phosphatase inhibitory activity, *Bioorg. Med. Chem. Lett. 13*, 2895−2898.
17. Wang, Q., Dube, D., Friesen, R. W., LeRiche, T. G., Bateman, K. P., Trimble, L., Sanghara, J., Pollex, R., Ramachandran, C., Gresser, M. J., and Huang, Z. (2004) Catalytic inactivation of protein tyrosine phosphatase CD45 and protein tyrosine phosphatase 1B by polyaromatic quinones, *Biochemistry 43*, 4294−4303.
18. Tjernberg, A., Hallen, D., Schultz, J., James, S., Benkestock, K., Bystrom, S., and Weigelt, J. (2004) Mechanism of action of pyridazine analogues on protein tyrosine phosphatase 1B (PTP1B), *Bioorg. Med. Chem. Lett. 14*, 891−895.
19. Salmeen, A., Andersen, J. N., Myers, M. P., Meng, T. C., Hinks, J. A., Tonks, N. K., and Barford, D. (2003) Redox regulation of protein tyrosine phosphatase 1B involves a sulphenyl-amide intermediate, *Nature 423*, 769−773.
20. van Montfort, R. L., Congreve, M., Tisi, D., Carr, R., and Jhoti, H. (2003) Oxidation state of the active-site cysteine in protein tyrosine phosphatase 1B, *Nature 423*, 773−777.
21. Meng, T. C., Buckley, D. A., Galic, S., Tiganis, T., and Tonks, N. K. (2004) Regulation of insulin signaling through reversible oxidation of the protein tyrosine phosphatases TC45 and PTP1B, *J. Biol. Chem. 279*, 37716−37725.
22. Tethering is a service mark of Sunesis Pharmaceuticals, Inc., for its fragment-based drug discovery.
23. Erlanson, D., Braisted, A., Raphael, D., Randal, M., Stroud, R., Gordon, E., and Wells, J. (2000) Site-directed ligand discovery, *Proc. Natl. Acad. Sci. U.S.A. 97*, 9367−9372.
24. Erlanson, D. A., Lam, J. W., Wiesmann, C., Luong, T. N., Simmons, R. L., DeLano, W. L., Choong, I. C., Burdett, M. T., Flanagan, W. M., Lee, D., Gordon, E. M., and O'Brien, T. (2003) In situ assembly of enzyme inhibitors using extended tethering, *Nat. Biotechnol. 21*, 308−314.
25. Erlanson, D. A., Wells, J. A., and Braisted, A. C. (2004) Tethering: Fragment-based drug discovery, *Annu. Rev. Biophys. Biomol. Struct. 33*, 199−223.
26. Barrett, W. C., DeGnore, J. P., Konig, S., Fales, H. M., Keng, Y.-F., Zhang, Z.-Y., Yim, M. B., and Chock, P. B. (1999) Regulation of PTP1B via glutathionylation of the active site cysteine 215, *Biochemistry 38*, 6699−6705.
27. Toyo'oka, T., and Imai, K. (1984) New fluorogenic reagent having halogenobenzofurazan structure for thiols: 4-(Aminosulfonyl)-7-fluoro-2,1,3-benzoxadizole, *Anal. Chem. 56*, 2461−2464.
28. Kirley, T. L. (1989) Determination of three disulfide bonds and one free sulfhyrdryl in the β-subunit of (Na,K)-ATPase, *J. Biol. Chem. 264*, 7185−7192.
29. Kirley, T. L. (1989) Reduction and fluorescent labeling of cyst(e)ine-containing proteins for subsequent structural analyses, *Anal. Biochem. 180*, 231−236.
30. Choi-Miura, N. H., Takahashi, Y., Nakano, Y., Tobe, T., and Tomita, M. (1992) Identification of the disulfide bonds in human plasma proteins SP-40,40 (apolipoprotein-J), *J. Biochem. 112*, 557−561.
31. Chin, C. C. Q., and Wold, F. (1993) The use of tributylphosphine and 4-(aminosulfonyl)-7-fluoro-2,1,3-benzoxadiazole in the study of protein sulfhydryls and disulfides, *Anal. Biochem. 214*, 128−134.
32. Toyo'oka, T., and Imai, K. (1985) Isolation and characterization of cysteine-containing regions of proteins using 4-(aminosulfonyl)-7-fluoro-2,1,3-benzoxadiazole and high-performance liquid chromatography, *Anal. Chem. 57*, 1931−1937.
33. Takeda, S., Yamaki, M., Ebina, S., and Nagayama, K. (1995) Site-specific reactivities of cysteine residues in horse L-apoferritin, *J. Biochem. 117*, 267−270.
34. Takeda, S., Arisaka, F., Ishii, S., and Kyogoku, Y. (1990) Structural studies of the contractile tail sheath protein of bacteriophage T4. 1. Conformational change of the tail sheath upon contraction as probed by differential chemical modification. *Biochemistry 29*, 5050−5056.
35. Hiratsuka, T. (1993) Behavior of Cys-707 (SH1) in myosin associated with ATP hydrolysis revealed with a fluorescent probe linked directly to the sulfur atom, *J. Biol. Chem. 268*, 24742−24750.
36. Luo, Y., Zhou, Y., and Cooperman, B. S. (1999) Antichymotrypsin interaction with chymotrypsin: Intermediates on the way to inhibited complex formation, *J. Biol. Chem. 274*, 17733−17741.
37. Maruta, S., Aihara, T., Uyehara, Y., Homma, K., Sugimoto, Y., and Wakabayashi, K. (2000) Solution structure of myosin-ADP-MgFn ternary complex by fluorescent probes and small-angle synchrotron X-ray scattering, *J. Biochem. 128*, 687−694.
38. Yang, Y., Maret, W., and Vallee, B. L. (2001) Differential fluorescence labeling of cysteinyl clusters uncovers high tissue levels of thionein, *Proc. Natl. Acad. Sci. U.S.A. 98*, 5556−5559.

39. Liu, R., and Sharom, F. J. (1998) Proximity of the nucleotide binding domains of the P-glycoprotein multidrug transporter to the membrane surface: A resonance energy transfer study, *Biochemistry 37*, 6503−6512.
40. Wiesmann, C., Barr, K. J., Kung, J., Zhu, J., Erlanson, D. A., Shen, W., Fahr, B. J., Zhong, M., Taylor, L., Randal, M., McDowell, R. S., and Hansen, S. K. (2004) Allosteric inhibition of protein tyrosine phosphatase 1B, *Nat. Struct. Mol. Biol. 11*, 730−737.
41. Treuheit, M. J., and Kirley, T. L. (1993) Reversibility of cysteine labeling by 4-(aminosulfonyl)-7-fluoro-2,1,3-benzoxadiazole, *Anal. Biochem. 212*, 138−142.
42. Lauren, S. L., and Treuheit, M. J. (1998) Removal of the fluorescent 4-(aminosulfonyl)-2,1,3-benzoxadiazole label from cysteine-containing peptides, *J. Chromatogr., A 798*, 47−54.
43. Xie, L., Lee, S. Y., Andersen, J. N., Waters, S., Shen, K., Guo, X. L., Moller, N. P., Olefsky, J. M., Lawrence, D. S., and Zhang, Z. Y. (2003) Cellular effects of small molecule PTP1B inhibitors on insulin signaling, *Biochemistry 42*, 12792−12804.
44. Husted, L. B., Sorensen, E. S., and Sottrup-Jensen, L. (2003) 4-(Aminosulfonyl)-7-fluoro-2,1,3-benzoxadiazole is not specific for labeling of sulfhydryl groups in proteins as it may also react with phenolic hydroxyl groups and amino groups, *Anal. Biochem. 314*, 166−168.
45. Zhang, Z. Y., and Dixon, J. E. (1993) Active site labeling of the *Yersinia* protein tyrosine phosphatase: The determination of the pK_a of the active site cysteine and the function of the conserved histidine 402, *Biochemistry 32*, 9340−9345.
46. Andersen, J. N., Mortensen, O. H., Peters, G. H., Drake, P. G., Iversen, L. F., Olsen, O. H., Jansen, P. G., Andersen, H. S., Tonks, N. K., and Moller, N. P. (2001) Structural and evolutionary relationships among protein tyrosine phosphatase domains, *Mol. Cell. Biol. 21*, 7117−7136.
47. Flint, A. J., Tiganis, T., Barford, D., and Tonks, N. K. (1997) Development of "substrate-trapping" mutants to identify physiological substrates of protein tyrosine phosphatases, *Proc. Natl. Acad. Sci. U.S.A. 94*, 1680−1685.
48. Patel, J. M., Zhang, J., and Block, E. R. (1996) Nitric oxide-induced inhibition of lung endothelial cell nitric oxide synthase via interaction with allosteric thiols: Role of thioredoxin in regulation of catalytic activity, *Am. J. Respir. Cell Mol. Biol. 15*, 410−419.
49. Chiadmi, M., Navaza, A., Miginiac-Maslow, M., Jacquot, J. P., and Cherfils, J. (1999) Redox signalling in the chloroplast: Structure of oxidized pea fructose-1,6-bisphosphate phosphatase, *EMBO J. 18*, 6809−6815.
50. Arrigo, A. P. (1999) Gene expression and the thiol redox state, *Free Radical Biol. Med. 27*, 936−944.
51. Marshall, H. E., Merchant, K., and Stamler, J. S. (2000) Nitrosation and oxidation in the regulation of gene expression, *FASEB J. 14*, 1889−1900.
52. Walsh, G. M., Sheehan, D., Kinsella, A., Moran, N., and O'Neill, S. (2004) Redox modulation of integrin $\alpha_{IIb}\beta_3$ involves a novel allosteric regulation of its thiol isomerase activity, *Biochemistry 43*, 473−480.
53. Hardy, J. A., Lam, J., Nguyen, J. T., O'Brien, T., and Wells, J. A. (2004) Discovery of an allosteric site in the caspases, *Proc. Natl. Acad. Sci. U.S.A. 101*, 12461−12466.
54. Barford, D., Flint, A. J., and Tonks, N. K. (1994) Crystal structure of human protein tyrosine phosphatase 1B, *Science 263*, 1397−1404.
55. DeLano, W. L. (2004) *PyMOL*, http://pymol.sourceforge.net/.

BI047417S